

A NOVEL LEARNING BASED SEGMENTATION METHOD FOR RODENT BRAIN STRUCTURES USING MRI

Jinghao Zhou¹, Sukmoon Chang^{1,2}, Qingshan Liu¹, George Pappas³, Vasilios Boronikolas³, Michael Michaelides³, Nora D. Volkow³, Panayotis K. Thanos³, Dimitris Metaxas¹

¹ CBIM, Rutgers, The State University of New Jersey, Piscataway, NJ, USA

² Computer Science, Capital College, Penn State University, Middletown, PA, USA

³ Behavior Neuropharmacology and Neuroimaging Lab, Medical Department, Brookhaven National Laboratory, Upton, NY, USA

ABSTRACT

This paper reports a novel method for fully automated segmentation of rodent brain volume by extending the robust active shape models to incorporate an automatic prior shape selection process. This automatic prior shape selection process using support vector machines provides an automatic shape initialization method for further segmentation of rodent brain structures such as Cerebellum, Neocortex, Corpus Callosum, External Capsule, Caudate Putamen, Hippocampus and Ventricles with the robust active shape model framework in magnetic resonance images (MRI). The mean successful rate of this classification method shows 92.2% accuracy compared to the expert-defined ground truth. We also demonstrate the very promising segmentation results of the robust active shape model framework in rodent brain volume.

Index Terms— Biomedical image processing, Image segmentation, Learning systems, Robust active shape model

1. INTRODUCTION

Segmentation of 3D brain images is very important to advance knowledge about relationships between anatomy and mental diseases in brains [1]. Volumetric analysis of rodent brain structures, such as, cerebellum, caudate putamen, hippocampus, fibria, external capsule and neocortex are important in studying the structural changes occurring in specific brain regions as a function of development, trauma or neurodegeneration [2]. Volumetric analysis of gray matter (GM), white matter (WM) and cerebrospinal fluid (CSF) is used to characterize morphological differences between subjects in psychiatric disease including schizophrenia, epilepsy or Alzheimer's disease [3, 4].

Currently, many semi-automatic and automatic segmentation methods in clinical studies have been developed [5, 6, 7, 8, 9], since manual segmentation of brain images are time-consuming and lack the reproducibility because of a large intra-observer and inter-observer variability. Pitiot et al. developed an expert-knowledge guided segmentation system for

anatomical structures in MRI which uses medical expertise in the form of implicit or explicit knowledge [5]. Leventon et al. presented a method of incorporating shape information into the image segmentation process [6]. Barra and Boire combined medical expertise with fuzzy maps using information fusion to segment anatomical structures in brain MRIs [7]. Niessen et al. presented an MRI brain segmentation method which combines an edge dependent multiscale representation with an intensity based linking scheme [8]. Shen et al. presented an adaptive deformable model for automatically segmenting brain structures from volumetric MR images [9].

Miscellaneous approaches have been applied to segment volume from all above papers. We will apply learning methods which can utilize autonomous acquisition and integration of knowledge to develop an automatic prior shape selection process. The goal of this paper is to develop an automatic brain structure segmentation method from 3D rodent brain MRIs by extending the robust active shape models to incorporate an automatic prior shape selection process. The proposed method first builds a set of priori shapes for each brain structure. Then, by classifying the brain structures present in a given image using a machine learning method (in section 2.1), it quickly selects a set of prior shapes and constructs a composite model by combining the selected priori shape models (in section 2.2). The composite model is automatically initialized (in section 2.3) and then deformed to fit to the corresponding brain structures using the active shape model (ASM) framework with significant improvements (in section 2.4). The method presented in this paper was specif-

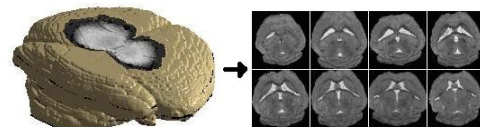


Fig. 1. 3D mouse brain volume and its unfolded 2D slices.

ically developed for segmentation of mouse brain structures in 3D brain images. However, it is generally applicable to any task involving deformable shape analysis of objects that change their topological structures in a given dataset.

2. METHOD

2.1. Automatic prior shape selection

As shown in Fig. 1, if we unfold the 3D mouse brain volume into 2D slices, we can see that the topology of the brain structures vary with the slice positions. According to experts [2], these variations of brain structures can be classified as five classes (see Fig. 2) and each class contains different combinations of different brain structures. To classify brain images into 5 classes, we specifically consider the following structures of the mouse brain: Cerebellum (S1), Neocortex (S2), Corpus Callosum & External Capsule (S3), Caudate Putamen (left: S4; right: S5), Hippocampus (left: S6; right: S7), Lateral Ventricles (left front: S8; right front: S9; left rear: S10; right rear: S11), Third Ventricle (S12) and Fourth Ventricle (S13). All regions of interest were selected by experts and were based on a stereotaxic rodent brain atlas [10]. Among these component brain structures, class 1 (C1) contains S1, S2, S3, S8, S9 and S13. Class 2 (C2) contains S1, S2, S3, S8, S9, S12 and S13. Class 3 (C3) contains all structures except S10 and S11. Class 4 (C4) contains all structures. Class 5 (C5) contains all structures except S1 and S3.

Given a slice, if we know which class it belongs to, we can get proper prior shape information for further ASM segmentation. In this paper, we use Support Vector Machines (SVM) [11] to deal with this task of classification. SVM has been known for its successes in many pattern recognition applications [12]. Its idea is first to project the input data into an implicit feature space F , i.e., $x \in R^N \rightarrow \Phi(x) \in F$ with the kernel trick, and then find the optimum decision hyper-plane in F to maximize the margins between two classes. In implementation, the kernel trick does not need to compute the implicit feature $\Phi(x)$ explicitly and the dot product of two implicit features $\Phi(x_1)$ and $\Phi(x_2)$ can be written as a kernel function $k(x_1, x_2)$. Given a sample x , its label predicted by SVM is given by the following:

$$f(x) = \text{sign}\left(\sum_{i=1}^n y_i a_i k(x, x_i) + b\right)$$

where x_i , $i = 1, 2, \dots, n$ are the training samples, $y_i = \{1, -1\}$ represents the label of the training samples, the coefficients a_i and b are the solutions of a quadratic programming problem. The training samples with non-zero a_i are called the support vectors [13].

There are several popular kernels. In our experiments, we use the Gaussian Radial Basis Function as the kernel: $k(x_1, x_2) = \exp(-\gamma \|x_1 - x_2\|^2)$. The classical SVM is a



Fig. 2. Five classes of mouse brain images based on the different brain structures present in the images

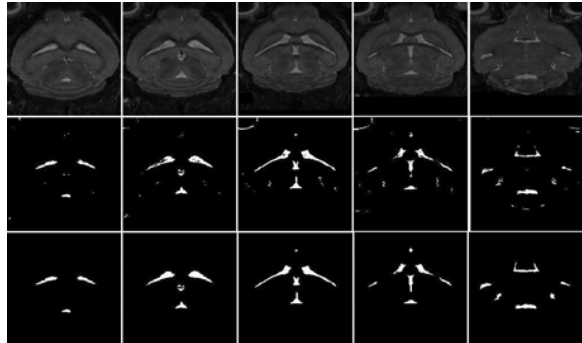


Fig. 3. The results of the coarse segmentation for automatic and accurate initialization of the ASM.

typical binary classifier. In this paper, we adopt one-to-all strategy to handle the multi-class problem.

2.2. Active shape models and their limitation

An active shape model represents the features of a shape as the point distribution model (PDM) [14]. Given a set of training images, the feature of interest in each image is manually labeled with n landmark points and represented as a vector in $2n$ -dimensional space, i.e., $x = \langle x_0, y_0, x_1, y_1, \dots, x_{n-1}, y_{n-1} \rangle$. After aligning these vectors into a common coordinate system, a set of orthogonal bases P is computed with the principal component analysis. Then, each aligned shape can be reconstructed as $x = \bar{x} + Pb$, where \bar{x} and b are the mean shape and the shape parameter vector, respectively. This equation also allows us to search for a new example of the shape in an unlabeled image by varying b appropriately, often based on low-level image features such as the gradients along normal directions to the boundary of an initial shape toward the strongest edge in the image. Although it has been used successfully in many applications, ASM has two important limitations for the segmentation of brain structures in MRI. In the next two sections, we will address these limitations and propose methods to overcome these drawbacks.

2.3. Automatic initialization of ASM

The major drawback of ASM for searching for a new example of the shape in an unlabeled image is the initialization of the

model. If the model is initialized too far from the feature of interest, the process may fail. To automate the accurate initialization of the model, we first rapidly extract the ventricles areas from unlabeled images by applying a series of thresholding and morphological operators.

The coarse segmentation process is illustrated in Fig. 3. The given images in top row are first normalized and thresholded, using the 90% quantile intensity value of the normalized image as the threshold value, to generate a binary images shown in middle row. Then we applied a series of morphological operators to obtain the coarse segmentation of brain structures as shown in bottom row. Note that our interest at this step is not the accurate segmentation of the brain structures. The coarse brain structures obtained here are used only to automate the accurate initialization of the shape model on unlabeled images. We achieve the automatic and accurate initialization by aligning the centers of the shape models to the centers of the segmented coarse brain structures.

2.4. Robust active shape models

Another limitation of ASM in finding an object in unlabeled images is that it heavily relies on the low-level image features to guide the search for the optimal positions of the feature points. For example, the gradient descent search on the image intensity profile has been widely used to move the model points toward the strongest edge in the image [14]. However, this approach is not suitable for the accurate delineation of Cerebellum of the brain in MRI since Cerebellum is intensity non-uniformity with stripes occlude structures and appear as the strongest edge (Fig. 1). We overcome this difficulty by introducing a robust error function based on the M-estimator [15].

Given an orthogonal basis P obtained in Sec. 2.2, the projection C of a new example shape X is given by $C = P^T dX$, where $X = \bar{X} + dX$ and \bar{X} is the mean shape of the aligned shapes from the training images. Using the projection C , we can also find a corresponding shape as $\hat{X} = \bar{X} + PC$, in which \hat{X} and PC approximates X and dX , respectively. Therefore, instead of obtaining X by optimizing dX using low-level image features only, our goal is to find the optimal C by minimizing the following robust energy function:

$$E_{rpca}(C) = \rho(\|dX - PC\|, \sigma)$$

where, $\rho(x, \sigma) = x^2 / (x^2 + \sigma^2)$ is the Geman-McClure error function and σ is a scale parameter that controls the convexity of the robust function. With an iterative gradient descent search on E , we get:

$$C^{(n+1)} = C^{(n)} + \lambda \Delta C$$

where, λ is a small constant that determines the step size and

$$\Delta C = \frac{\partial E_{rpca}}{\partial C} = -2P(dX - PC) \frac{\sigma^2}{(\|dX - PC\|^2 + \sigma^2)^2}$$



Fig. 4. MR image of the brain with landmarks of brain structures superimposed of each class.

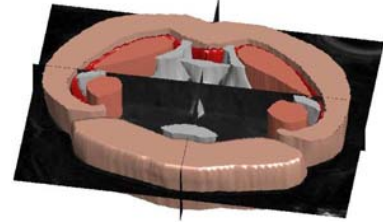


Fig. 5. 3D reconstruction of segmentation result.

By continuing the iterative process until $\|E^{(n+1)} - E^{(n)}\| < \varepsilon$, where ε is a preselected tolerance, we obtain the optimal project C and a robust shape in the shape space as:

$$\hat{X} = \bar{X} + PC$$

The results of this process are illustrated in Fig. 4, where the Cerebellum occluded by the strips are accurately segmented.

3. RESULTS

Six 4-month-old mice were anesthetized with ketamine/xylozine mixture (100mg/kg/10mg/kg) and placed inside a 9.4T MR scanner [16]. Each mouse brain scan generated a 3D gradient echo (GE) image volume acquired at high resolution (50x50x50-micron isotropic resolution). The images of all mice were segmented manually using the AMIRA software environment by experts.

To test the proposed classification method, we randomly sampled 50 patches for each image; in total, we generated 5000 training images (1000 images per class) and 3250 testing images (class 1: 650, class 2: 750, class 3: 600, class 4: 600, class 5: 650). The mean successful rate of the multiple classes of the testing data is 92.2%.

Then we automatically segmented all testing images using the robust ASM method as described in Section 2.3 and 2.4. Fig. 4 shows the automatic segmentation result and its 3D reconstruction (Fig. 5). The ASM method encodes for each structure of the brain that we want to segment the statistical variation of its shape and its appearance along the shape boundaries. Table 1 shows the mean overlap ratios of structures of different classes of brain volume between the ground truth and the ASM segmented images.

Mean overlap ratio	C1	C2	C3	C4	C5
S1	0.9887	0.9789	0.9643	0.9837	N/A
S2	0.9867	0.9764	0.9717	0.9623	0.9756
S3	0.6874	0.7462	0.5945	0.6390	N/A
S4	N/A	N/A	0.8752	0.8546	0.8358
S5	N/A	N/A	0.9043	0.8958	0.8680
S6	N/A	N/A	0.8627	0.8745	0.8297
S7	N/A	N/A	0.8519	0.8913	0.8473
S8	0.9877	0.9783	0.9794	0.9848	0.9736
S9	0.9852	0.9836	0.9755	0.9809	0.9741
S10	N/A	N/A	N/A	0.9786	0.9866
S11	N/A	N/A	N/A	0.9839	0.9742
S12	N/A	0.9655	0.9539	0.9678	0.9438
S13	0.9342	0.9434	0.9712	0.9509	0.9642

Table 1. Mean overlap ratios of structures of different classes of brain volume between the ground truth and the ASM segmented images. C1 to C5 are defined classes. S1 to S13 are different brain structures.

4. CONCLUSION

We proposed a novel method for fully automated segmentation of 3D mouse brain volume that is based on the extended robust active shape models by incorporating an automatic prior shape selection process. The automatic prior shape selection process using support vector machines classifies the 3D mouse brain volume into multiple classes corresponding to the topological changes of brain structures. With these promising results, the method can be used to provide a high throughput automatic segmentation of rodent brains for many different preclinical neuroscience applications.

5. REFERENCES

- [1] A. Pitiot, H. Delingette, and P.M. Thompson, *Medical Image Systems: Technology and Applications*, chapter Automated Image Segmentation: Issues and Applications, Academic Press, 2004.
- [2] V. Boronikolas, M. Michaelides, J. Zhou, G.J. Wang, S. Blackband, S. Grant, D. Metaxas, N. Volkow, and P.K. Thanos, "Validation of the active shape model for automatic brain region segmentation," *IEEE Nuclear Science Symposium and Medical Imaging Conference*, 2006.
- [3] R.W. McCarley, C.G. Wiblea, M. Frumina, Y. Hirayasu, J.J. Levitta, I.A. Fischera, and M.E. Shenton, "Mri anatomy of schizophrenia," *Biological Psychiatry*, vol. 45, no. 9, pp. 1099–1119, 1999.
- [4] O.T. Carmichael, H.A. Aizenstein, S.W. Davis, J.T. Becker, P.M. Thompson, C.C. Meltzer, and Y. Liu, "Atlas-based hippocampus segmentation in alzheimer's disease and mild cognitive impairment," *NeuroImage*, vol. 27, no. 4, pp. 979–990, 2005.
- [5] A. Pitiot, H. Delingette, P.M. Thompson, and Ayache N., "Expert knowledge-guided segmentation system for brain mri," *NeuroImage*, vol. 23, pp. s85–s96, 2004.
- [6] M. Leventon, E. Grimson, and O. Faugeras, "Statistical shape influence in geodesic active contours," *IEEE Proc. of Computer Vision and Pattern Recognition*, pp. 4–11, 2000.
- [7] V. Barra and J.Y. Boire, "Automatic segmentation of subcortical brain structures in mr images using information fusion," *IEEE transactions on medical imaging*, vol. 20, no. 7, pp. 549–558, 2001.
- [8] W.J. Niessen, K.L. Vincken, J. Weickert, B.M.T.H. Romeny, and M.A. Viergever, "Multiscale segmentation of three-dimensional mr brain images," *International Journal of Computer Vision*, vol. 31, no. 2, pp. 185–202, 1999.
- [9] D. Shen, E.H. Herskovies, and C. Davatzikos, "An adaptive-focus statistical shape model for segmentation and shape modeling of 3d brain structures," *IEEE Transactions on Medical Imaging*, vol. 20, no. 4, pp. 257–270, 2001.
- [10] G. Paxinos and C. Watson, *The Rat Brain in Stereotaxic Coordinates*, Academic Press, second edition edition, 1986.
- [11] V.S. Cherkassky and F. Mulier, *Learning from Data: Concepts, Theory, and Methods*, Wiley, 1998.
- [12] R. Duda, P.E. Hart, and D.G. Stork, *Pattern Classification*, 2000.
- [13] E. Osuna, R. Freund, and Girosi F., *Support Vector Machines: Training and Applications*, Tech Report, AI Lab, MIT, second edition edition, 1997.
- [14] T. Cootes, C. Taylor, D. Cooper, and J. Graham, "Active shape models-their training and application," *Computer Vision and Image Understanding*, vol. 61, no. 1, pp. 38–59, 1995.
- [15] F. De La Torre and M. Black, "A framework for robust subspace learning," *International Journal of Computer Vision*, vol. 54, no. 1-3, pp. 117–142, 2003.
- [16] P.K. Thanos, M. Michaelides, H. Benveniste, G.J. Wang, and N.D. Volkow, "The effects of cocaine on regional brain glucose metabolism is attenuated in dopamine transporter knockout mice," *Synapse*, vol. 62, pp. 319–324, 2008.